View metadata, citation and similar papers at core.ac.uk
brought to you by CORE
provided by St Andrews Research Repository

Unipolar resistive switching in planar Pt/BiFeO3/Pt structure

Rajesh K. Katiyar, Yogesh Sharma, Danilo G. Barrionuevo Diestra, Pankaj Misra, Sudheendran Kooriyattil, Shojan P. Pavunny, Gerardo Morell, Brad R. Weiner, J. F. Scott, and Ram S. Katiyar

Citation: AIP Advances **5**, 037109 (2015); doi: 10.1063/1.4914475
View online: http://dx.doi.org/10.1063/1.4914475
View Table of Contents: http://scitation.aip.org/content/aip/journal/adva/5/3?ver=pdfcov
Published by the AIP Publishing

Articles you may be interested in

Study of resistive switching and magnetism modulation in the Pt/CoFe2O4/Nb:SrTiO3 heterostructures
Appl. Phys. Lett. **107**, 063502 (2015); 10.1063/1.4928337

Ferroelectric memristor based on Pt/BiFeO3/Nb-doped SrTiO3 heterostructure
Appl. Phys. Lett. **102**, 102901 (2013); 10.1063/1.4795145

Evolution of the resistive switching in chemical solution deposited-derived BiFeO3 thin films with dwell time and annealing temperature
J. Appl. Phys. **113**, 043706 (2013); 10.1063/1.4789265

Nonpolar resistive switching in Mn-doped BiFeO3 thin films by chemical solution deposition
Appl. Phys. Lett. **101**, 062902 (2012); 10.1063/1.4742897

Nonvolatile bipolar resistive switching in Au/BiFeO3/Pt
J. Appl. Phys. **109**, 124117 (2011); 10.1063/1.3601113

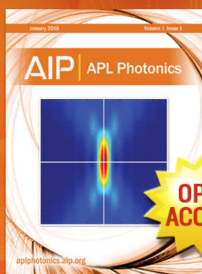

Launching in 2016!
The future of applied photonics research is here
AIP APL Photonics

Reuse of AIP Publishing content is subject to the terms at: https://publishing.aip.org/authors/rights-and-permissions. IP: 138.251.162.214 On: Fri, 19 Feb 2016 11:29:10

AIP ADVANCES 5, 037109 (2015)

Unipolar resistive switching in planar Pt/$BiFeO_3$/Pt structure

Rajesh K. Katiyar,[1,2,a] Yogesh Sharma,[1,2] Danilo G. Barrionuevo Diestra,[1,2] Pankaj Misra,[1,2] Sudheendran Kooriyattil,[1,2] Shojan P. Pavunny,[1,2] Gerardo Morell,[1,2] Brad R. Weiner,[1,3] J. F. Scott,[4] and Ram S. Katiyar[1,2]
[1]*Institute of Functional Nanomaterials, University of Puerto Rico, San Juan, PR 00931, USA*
[2]*Department of Physics, University of Puerto Rico, San Juan, Puerto Rico, PR 00936, USA*
[3]*Department of Chemistry, University of Puerto Rico, San Juan, PR 00936, USA*
[4]*Cavendish Laboratory, Department of Physics, University of Cambridge, CB0 3HE, United Kingdom*

(Received 26 September 2014; accepted 21 February 2015; published online 6 March 2015)

We report unipolar resistive switching suitable for nonvolatile memory applications in polycrystalline $BiFeO_3$ thin films in planar electrode configuration with non-overlapping Set and Reset voltages, On/Off resistance ratio of $\sim 10^4$ and good data retention (verified for up to 3,000 s). We have also observed photovoltaic response in both high and low resistance states, where the photocurrent density was about three orders of magnitude higher in the low resistance state as compared to the high resistance state at an illumination power density of ~ 100 mW/cm^2. Resistive switching mechanisms in both resistance states of the planar device can be explained by using the conduction filament (thermo-chemical) model. © *2015 Author(s). All article content, except where otherwise noted, is licensed under a Creative Commons Attribution 3.0 Unported License.* [http://dx.doi.org/10.1063/1.4914475]

I. INTRODUCTION

The resistive random access memory (ReRAM) with its simple design, excellent scalability, high speed storage capacity, low power consumption, and semiconductor process flow compatibility has been identified by ITRS[1] as a potential memory technology. The memory effect in ReRAM is realized through reversible switching of the resistance of a material between two conductive states, High Resistance State (HRS = Off) and Low Resistance State (LRS = On), when an adequate electrical signal (voltage or current) is applied across it. Initially, the application of a high voltage known as forming voltage switches the resistance of the device from HRS to LRS by the controlled breakdown at a limited current compliance.[2] After the forming process is complete, the memory cell is switched back to HRS by applying a threshold voltage (Reset). Once in HRS, the memory cell can again be switched to LRS simply by voltage sweep keeping the current compliance constant. Thus, the resistance of the memory cell can be switched repeatedly between the two states of low and high resistances provided the current compliance is correctly set.[3,4] Generally, the observed resistive switching behavior falls into two different classes depending on the polarity of the applied electrical stimulus, namely, bipolar resistive switching and unipolar resistive switching.[5] In the case of unipolar resistive switching, the Set and Reset processes occur by the same bias polarity,[6] whereas in bipolar resistive switching the Reset process requires a voltage bias opposite to that of the Set process.[7,8] Among the two, unipolar resistive switching is of particular importance as it offers higher contrast between the resistances of the two states.

Recently, bipolar resistive switching phenomenon was observed in well known multiferroic material $BiFeO_3$ (BFO) and its variants, receiving tremendous attention due to their potential in

[a]Corresponding Author Email: rajesh_katiyar3006@yahoo.com

 ©Author(s) 2015

Reuse of AIP Publishing content is subject to the terms at: https://publishing.aip.org/authors/rights-and-permissions. IP: 138.251.162.214 On: Fri, 19 Feb 2016 11:29:10

developing futuristic multifunctional nonvolatile memory devices combining ferroelectricity, ferromagnetism and photovoltaic effects.[9] Yao *et al.*[10,11] have reported bipolar resistive switching in epitaxial BFO thin films grown on single-crystal substrates. However, the ratio of two resistance states (high and low) was limited to ∼100 due to large leakage currents. Yin *et al.*[12] also have described bipolar resistive switching in polycrystalline BFO thin films with poor contrast in resistance ratio and the switching mechanism was found to be different from that of epitaxial thin films. Wang *et al.*[13] and Qu *et al.*[14] have observed bipolar resistance switching in $BiFeO_3$/Nb-$SrTiO_3$ heterojunctions with a contrast of ∼100 between the two resistance states and found substantial photovoltaic effect when the device was illuminated with white light. In most of these studies on resistive switching in BFO thin films, a metal-insulator-metal (MIM) type of structure with the insulating thin film sandwiched between two metallic electrodes was used and current-voltage measurements were done in top-bottom configuration. Moreover, prominent photovoltaic effect in BFO films exhibiting large open circuit voltage has been reported in planar electrode configuration, where both the metal electrodes are on the surface of BFO film.[15–18] Nonetheless, studies on the resistance switching phenomenon in BFO in planar electrode configuration and its effect on photovoltaic properties are missing in literature. In this work we report the unipolar resistance switching in polycrystalline BFO thin films configured in planar electrode geometry and the photovoltaic response associated with the two resistance states. Our studies show that BFO thin films can simultaneously act as memory devices (resistive memory effect) as well as an efficient energy harvester (ferroelectric photovoltaic effect) when configured in planar geometry.

II. EXPERIMENTAL

Polycrystalline BFO films of about 200 nm thickness were deposited by radio frequency (RF) sputtering technique on pulsed laser coated buffer layer of $SrRuO_3$ (SRO) on Pt/TiO_2/SiO_2/Si substrates kept in a mixture of argon and oxygen ambient (flow ratio of ∼5:2) in deposition chamber and at a temperature of ∼675 °C. The SRO buffer layer (∼100 nm thick) was first deposited at ∼600 °C substrate temperature and ∼80 mTorr oxygen pressure utilizing a KrF excimer laser($\lambda \sim 248$ nm). The phase formation of BFO thin films were confirmed by X-ray diffraction (XRD) and Raman studies. The XRD measurements were carried out using an automated Rigaku D/max 2400 X-ray diffractometer using the CuKα radiation. The Raman measurements were performed using an ISA T64000 triple monochromator. Circular platinum metal top electrodes of thickness ∼75 nm and diameter ∼200 µm were DC magnetron sputtered at a power density of ∼1 W/cm^2 to form symmetric co-planar devices. Ferroelectric nature of films was recorded using a Veeco Piezoresponse Force Microscope (PFM). The resistance switching characteristics of devices were studied through current-voltage (I-V) measurements in between the electrodes using a Keithley 2401 electrometer. Bias polarity was defined in between electrodes for the study of resistive switching in planar geometries. The photoresponse of BFO/SRO films in low and high resistance states were measured set at an illumination of ∼100 mW/cm^2 by utilizing a solar simulator (ABETS model 3000).

III. RESULTS AND DISCUSSION

The XRD pattern of the BFO thin films show their polycrystalline phase (Fig. 1(a)). All the peaks were indexed on the basis of a rhombohedral cell (JCPDS: 74-2016). Out of the eight observed Raman active modes in the spectral window of 10-700 cm^{-1} (Fig. 1(b)), the modes at 140.2 cm^{-1}, 171.1 cm^{-1} and 215.8 cm^{-1} are of A_1 symmetry, and those at 75.3 cm^{-1}, 260.7 cm^{-1}, 414.5 cm^{-1}, 467.7 cm^{-1}, 524.5 cm^{-1} and 606.1 cm^{-1} belong to E symmetry and confirmed the rhombohedral structure.[19]

The sharp contrast observed in PFM image as the polarization was switched back and forth demonstrates the ferroelectric nature of the films as shown in the inset of Fig. 1(b). The current-voltage (I-V) characteristics of symmetric planar BFO (MIM) devices are illustrated in Fig. 2. Memory cells containing platinum (Pt) electrodes having a separation of ∼100 µm were used to

Reuse of AIP Publishing content is subject to the terms at: https://publishing.aip.org/authors/rights-and-permissions. IP: 138.251.162.214 On: Fri, 19 Feb 2016 11:29:10

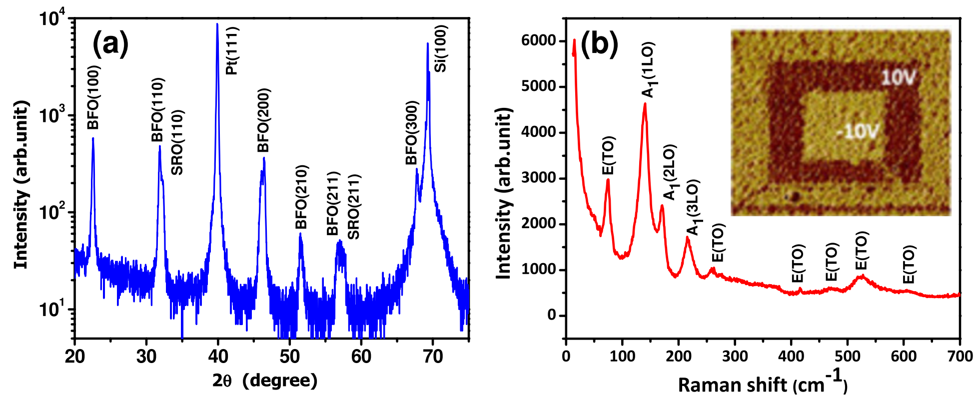

FIG. 1. (a) Room temperature XRD diffractogram and (b) Raman spectra of BFO thin films on SRO coated $Pt/TiO_2/SiO_2/Si$ substrate. Piezoresponse Force Microscope image of BFO thin films with an applied tip DC bias voltage of ±10V over a $10\times10\ \mu m^2$ area is shown in the inset of Fig. 1(b).

study the resistive switching behavior. Initially, a high resistance of ~1 MΩ was measured for the memory cells at an applied bias of ~0.1 V, which were then switched to a low resistance state when the applied bias voltage was increased to ~5.5 V. At this voltage, the resistance of the BFO films dropped abruptly to a low value of ~15 Ω (measured at ~0.1 V), as shown in Fig. 2(a). This is known as the initial forming process that converts the device from initial HRS into LRS. During the forming process, the current compliance was set at 20 mA to produce a controlled dielectric breakdown, thus preventing the failure of the device. Once the forming process is over, the device is switched back from LRS to HRS (termed as Reset process) accompanied by a sudden drop in current by the application of comparatively lower voltages (Reset voltage) without setting any limit to the current that flows through the dielectric BFO. Following the Reset process, the device is switched from HRS to LRS by the application of a comparatively higher voltage of the same polarity as the Set voltage and with a current limit similar to that of the forming process. The corresponding schematic diagram based on the conduction filamentary model is shown in the inset of Fig. 2(a). This Set-Reset process was found to be reversible and reproducible after repeated programming cycles. In planar geometry of BFO, the Set and Reset voltage window was observed in the range of ~0.75-1.5 V and ~3-3.5 V, respectively, as shown in Fig. 2(b). The observed memory effect is unipolar in nature as the resistive switching behavior of these devices is found to be independent of the polarity of the applied voltage.

In order to understand the switching mechanism of the devices under investigation, we measured the resistance in both HRS and LRS states as a function of temperature in the range of 300 – 475 K

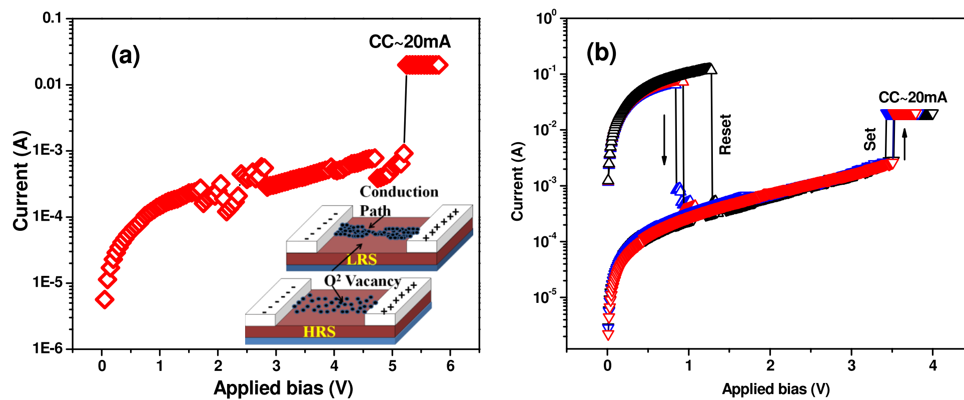

FIG. 2. Current-Voltage (I-V) characteristics of the planar BFO device showing: (a) forming and (b) Set-Reset processes. The inset shows the schematic diagram of the conduction filament model.

Reuse of AIP Publishing content is subject to the terms at: https://publishing.aip.org/authors/rights-and-permissions. IP: 138.251.162.214 On: Fri, 19 Feb 2016 11:29:10

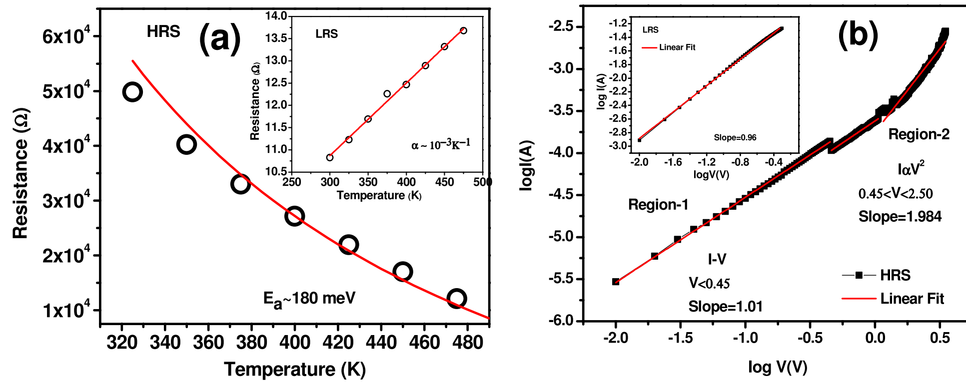

FIG. 3. (a) Temperature dependence of resistances in HRS. Inset of (Fig. 3(a)) shows the liner fit of resistance variation with temperature. Fig. 3(b) log I–log V curve for HRS of BFO in planar electrodes device showing two different regions with SCLC conduction mechanism. The inset shows log I–log V curve for LRS where the linear current–voltage relation indicates Ohmic conduction.

and the results are illustrated in Fig. 3(a). It can be seen in the inset of Fig. 3(a) that a metallic conduction behavior takes place in LRS with a reduction in resistance as the temperature increases, following the equation$R(T) = R(T_0)[1 + \alpha(T - T_0)]$, where, α is the temperature coefficient, T_0 is the reference temperature and $R(T_0)$ is the resistance at T_0. A straight line fit of the experimental data with this relation provided the linear temperature coefficient of BFO layer in LRS as $\sim 10^{-3}$ K^{-1}, which is a typical figure for electronic transport in metallic nanostructures.[20] In the case of HRS, as shown in Fig. 3(a), a semiconductor-like behavior was observed with the resistance decreasing exponentially with increasing temperature following the equation $R(T) = R(T_0)_e^{(E_a/k_B T)}$, where E_a is the thermal activation energy, k_B is the Boltzmann constant, and T is the temperature. The exponential fit of experimental data with the above relation provided an activation energy value of ~180 meV.

Based on the above analysis, it can be concluded that the resistance switching mechanism of symmetric planar BFO MIM devices follows the conductive filament model.[21] It has been widely discussed in BFO-perovskite that oxygen vacancies play crucial role in switching the conduction state of the film while applying an external field. In planar geometry, by applying positive voltage at one of the electrodes, oxygen ions start migrating towards this particular electrode and accumulate at the electrode/oxide interface, leaving behind a defect induced conductive path (made of oxygen vacancies) in between the planar electrodes, which sets the device to LRS (ON-state). Again sweeping the positive DC voltage during reset, at certain voltage (~1-1.5 V) the conducting path got ruptured due to the Joule-heating induced thermal migration of oxygen ions back to oxygen vacancies.[22] Therefore, the uniform switching between LRS and HRS of a dielectric material has been ascribed to the creation and subsequent rupture of conducting filaments which are a kind of extended defects (i.e., metallic precipitate and oxygen vacancies) distributed throughout the film.[23,24]

To clarify the conduction mechanism both in LRS and HRS of the BFO in planar electrode configuration, the I-V curves were re-plotted in log-log scale (Fig. 3(b)). It can be seen that in LRS (inset of Fig. 3(b)), the I-V plot is linear in the low voltage regime (< 0.6 V) with a slope of ~0.96, indicating metal-like Ohmic conduction. As can be seen in logarithmic I-V plot for HRS, two regimes were observed: one linear regime for smaller voltages (< 0.45 V), and the other for higher voltages (> 0.45 V) where a nonlinear increase in the current was observed. This kind of I-V behavior could be explained based on the space-charge-limited current conduction (SCLC) mechanism. On the basis of SCLC mechanism, the low voltage regime corresponds to Ohmic conduction ($I \propto V$), while in the high voltage regime the conduction is dominated by the Child's square law ($I \propto V^2$). The observed I-V behavior in HRS was found to be in better agreement with the SCLC charge transport mechanism.[25,26] Resistance state retention is excellent for both LRS (On) and HRS (Off) states, as they were measured to remain stable for at least 3000 seconds at room temperature (Figure not shown) confirming the nonvolatility of the programmed logic states.

Reuse of AIP Publishing content is subject to the terms at: https://publishing.aip.org/authors/rights-and-permissions. IP: 138.251.162.214 On: Fri, 19 Feb 2016 11:29:10

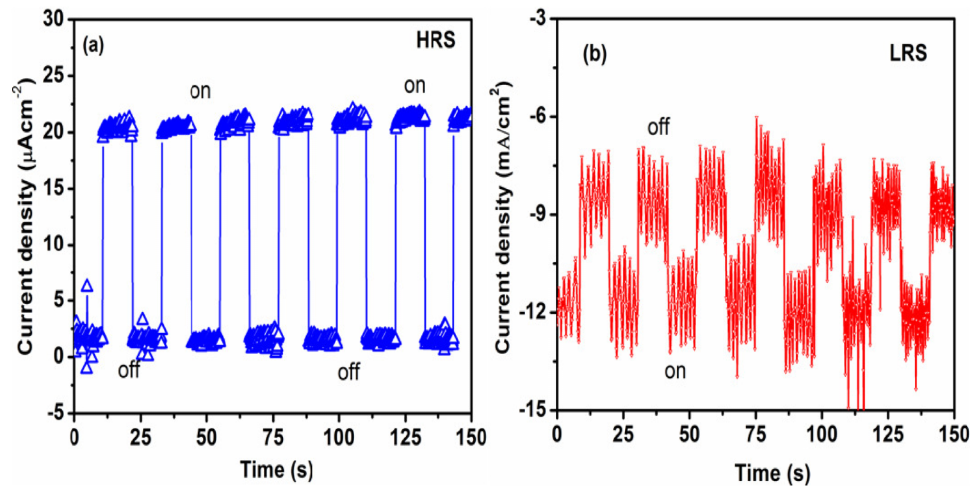

FIG. 4. Photoresponse of planar BFO structures in (a) HRS and (b) LRS.

It is also interesting to study the white-light PV effect in BFO thin films both in high and low resistance states. The time dependence of the photocurrent at zero bias voltage in LRS and HRS is shown in Fig. 4(a) and 4(b), respectively, when exposed to light. It can be seen that the PV On and Off states are repeatable and stable in both resistance states, confirming the efficient light harvesting effect. The open circuit current was found to be three orders of magnitude higher in LRS than in HRS, which is important for photovoltaic device applications.[27] However, it can be seen that in HRS the open circuit photocurrent is positive while it is negative in LRS at 0 V. The observed negative current in LRS of the planar Pt/BFO/Pt device could be due to the domain wall pinning or confinement at conducting filament,[28] When we apply DC voltage during reset process, the domains near the filament get reversed even at small voltages (~ 0.5-1 V) leaving the remaining the domain in the same polarization state. Probably, this polarization reversal leads to negative current when the device is exposed to white light illumination.

IV. CONCLUSIONS

In summary, the resistive switching properties and associated photocurrent response of BFO film with planar electrodes are reported. Repeatable and reliable non-volatile unipolar resistive switching behavior has been observed. The planar memory cell exhibited small and non-overlapping Set and Reset voltages, high resistance ratio of the two states ($\sim 10^4$) and good data retention for as long as 3000 s. The mechanism responsible for the resistive switching behavior was discussed in the light of the conduction filament model. Further, although PV response was also observed in both the low and high resistance states, the photo-current density was three orders of magnitude higher in LRS as compared to HRS at a white light illuminance of ~ 100 mW/cm^2.

ACKNOWLEDGMENTS

This work was supported by the NASA EPSCoR Grant # NNX13AB22A. Financial support to various researchers from IFN-NSF grant # EPS 1002410 (RSK, DB, YS and BRW) is gratefully acknowledged. S. K. is thankful to UGC, India for a Raman fellowship under Indo-US 21st century knowledge initiatives (No:5-53/2013(I.C)).

[1] *International Technology Roadmap for Semiconductors* (Semiconductor Industry Association, San Jose, CA, 2010), see http://www.itrs.net for updates.
[2] K. Kinoshita, T. Tamura, M. Aoki, Y. Sugiyama, and H. Tanaka, Appl. Phys. Lett. **89**, 103509 (2006).
[3] S. H. Baek, H. W. Jang, C. M. Folkman, Y. L. Li, B. Winchester, J. X. Zhang, Q. He, Y. H. Chu, C. T. Nelson, M. S. Rzchowski *et al.*, Nat. Mater **9**, 309 (2010).

Reuse of AIP Publishing content is subject to the terms at: https://publishing.aip.org/authors/rights-and-permissions. IP: 138.251.162.214 On: Fri, 19 Feb 2016 11:29:10

[4] D. S. Jeong, R. Thomas, R. S. Katiyar, J. F. Scott, H. Kohlstedt, A. Petraru, and C. S. Hwang, Rep. Prog. Phys. **75**, 076502 (2012).
[5] R. Chen, M. Lao, J. Xu, and C. Xu, Appl. Phys. Express. **7**, 095801 (2014).
[6] S. T. Zhang, M. H. Lu, D. Wu, Y. F. Chen, and N. B. Ming, Appl, Phys. Lett. **87**, 262907 (2005).
[7] R.K. Katiyar, P. Misra, G.L. Sharma, G. Morell, J.F. Scott, and R.S. Katiyar, Mater. Res. Soc. Symp. Proc. **1577** (2013) http://dx.doi.org/10.1557/opl.2013.702.
[8] Yogesh Sharma, Pankaj Misra, Shojan P. Pavunny, and Ram S Katiyar, Appl. Phys. Lett. **104**, 073501 (2014).
[9] A. Bhatnagar, A. R. Chaudhuri, Y. H. Kim, D. Hesse, and M. Alexe, Nat. Comm. **4**, 2835 (2013).
[10] Y. Yao, W. Liu, Y. Chan, C. Leung, C. Mak, and B. Ploss, Int. J. Appl. Ceram. Technol. **8**, 1246 (2011).
[11] L. Pintilie, C. Dragoi, Y. H. Chu, L. W. Martin, R. Ramesh, and M. Alex, Appl. Phys.Lett. **94**, 232902 (2009).
[12] K. Yin, M. Li, Y. Liu, C. He, F. Zhuge, B. Chen, W. Lu, X. Pan, and R. W. Li, Appl. Phys. Lett. **97**, 042101 (2010).
[13] C. Wang, K. Jin, Z. Xu, L. Wang, C. Ge, H. Lu, H. Guo, M. He and G. Yang, Appl. Phys. Lett. **98**, 192901 (2011).
[14] T. L. Qu, Y. G. Zhao, D. Xie, J. P. Shi, Q. P. Chen, and T. L. Ren, Appl. Phys. Lett. **98**, 173507 (2011).
[15] Y. Sharma, P. Misra, R. K. Katiyar, and R. S Katinar, J. Phys. D, Appl. Phys. **47**, 425303 (2014).
[16] S. Y. Yang, J. Seidel, S. J. Byrnes, P. Shafer, C.-H. Yang, M. D. Rossell, P. Yu, Y.-H. Chu, J. F. Scott, J. W. Ager III *et al.*, Nanotechnology **5**, 143 (2010).
[17] R. K. Katiyar, P. Misra, F. Mendoza, G. Morell, and Ram S. Katina, Appl. Phys. Lett. **105**, 142902 (2014).
[18] V. S. Puli, D. K. Pradhan, R. K. Katiyar, I. Coondoo, N. Panwar, P. Misra, D.B. Chrisey, J F Scott, and R. S. Katiyar, J. Phys. D: Appl. Phys. **47**, 075502 (2014).
[19] N. M. Murari, R. Thomas, R. E. Melgarejo, S. P. Pavunny, and R. S. Katiyar, J. Appl. Phys. **106**, 014103 (2009).
[20] D. Lee, S. H. Baek, T. H. Kim, J.G. Yoon, C. M. Folkman, C. B. Eom, and T. W. Noh, Phys. Rev. B. **84**, 125305 (2011).
[21] K Fujiwara, T. Nemoto, M. J. Rozenberg, Y. Nakamura, and H. Takagi, Jpn. J. Appl. Phys. **47**, 6266 (2008).
[22] K. Fujiwara, T. Nemoto, M. J. Rozenberg, Y. Nakamura, and H. Takagi, Jpn. J. Appl. Phys. **47**, 6266 (2008).
[23] Y. Sharma, S. Pavunny, E. Fachini, J. F. Scott, and R. S. Katiyar, J. Appl. Phys. (2015) (Under review).
[24] Y. P. Wang, L. Zhou, M. F. Zhang, X. Y. Chen, J. M. Liu, and Z. G. Liu, Appl. Phys. Lett. **84**, 1731 (2004).
[25] Yogesh Sharma, Pankaj Misra, and Ram S. Katiyar, J. Appl. Phys. **116**, 084505 (2014).
[26] D-Y. Lee and T-Y. Tseng, J. Appl. Phys. **110**, 114117 (2011).
[27] Z. Hu, Q. Li, M. Li, Q. Wang, Y. Zhu, X. Liu, X. Zhao, Yun Liu, and S. Dong, Appl. Phys. Lett. **102**, 102901 (2013).
[28] Kim *et al.*, ACS Appl. Mater. Interfaces **6**, 6346–6350 (2014).

Reuse of AIP Publishing content is subject to the terms at: https://publishing.aip.org/authors/rights-and-permissions. IP: 138.251.162.214 On: Fri, 19 Feb 2016 11:29:10